Journal of Animal Research: v.7 n.4, p. 653-660. August 2017

DOI: 10.5958/2277-940X.2017.00100.0

Morphological and Histochemical Characteristics of Parotid Salivary Gland in Neonates of Indian Buffalo

Aman Deep Singh[1]* and Opinder Singh[2]

[1]Department of Veterinary Anatomy, College of Veterinary Sciences, Lala Lajpat Rai University of Veterinary and Animal Sciences, Hisar, Haryana, INDIA

[2]Department of Veterinary Anatomy, College of Veterinary Sciences, Guru Angad Dev Veterinary and Animal Sciences University, Ludhiana, Punjab, INDIA

**Corresponding author: AD Singh; Email: amanatomy287@gmail.com*

Received: 15 March, 2017 **Revised:** 04 June, 2017 **Accepted:** 14 June, 2017

ABSTRACT

The present study was aimed to elucidate gross, histomorphological and histochemical status in parotid salivary gland of buffalo during neonatal life. The study was carried out on parotid salivary gland of eighteen buffalo neonates. These neonates were categorized into three groups based on their age, viz., Group-1: <1 month; Group-2: between1-2 months and Group-3: between 2-3 months. Macroscopically, the lateral surface of the gland was covered by parotid fascia, developing parotido-auricularis muscle and facial muscles and the medial surface was related to great cornu of hyoid bone, digastricus, occipito-hyoideus and sterno-mastoideus muscles, external carotid artery, external jugular vein and its tributaries, facial nerve and its branches, during early neonatal life. Histologically, the parotid gland was of compound tubuloacinar nature. The parenchyma comprised of purely serous acini along with several orders of ducts distributed in the stroma. The duct system comprised of intercalated duct, striated duct, interlobular duct and large excretory duct. The myoepithelial cells appeared as flattened basal cells initially around the developing acinar cells. The serous acinar cells of parotid gland were devoid of acidic and neutral mucopolysaccharides in neonatal age groups. Fine lipid droplets were observed in intralobular as well as interlobular connective tissue. The biometrical studies showed that there was a significant difference in the parotid gland between different neonatal age groups at $p \leq 0.05$ and $p \leq 0.01$ level. There was significant difference in the micrometrical parameters of parotid gland between different groups at $p \leq 0.05$ and $p \leq 0.01$ level.

Keywords: Biometry, Buffalo, Histomorphology, Histochemistry, Neonatal, Parotid salivary gland.

The oral cavity is underlined by a mucosal membrane and is always moistened by the saliva secreted by the associated major and minor salivary glands. Major salivary glands consist of three pairs of macroscopic glandular organs i.e., parotid, submandibular and sublingual (Amano, 2011). These glands secrete serous, mucous or mixed saliva via the proper main excretory ducts connecting the glandular bodies with the oral cavity. In ruminants, the minor salivary glands (buccal, labial etc.) are named according to their location, although the saliva secretion is small in quantity compared with the major ones (Singh *et al.,* 2012). The broader distributions of the minor salivary glands are advantageous for the protection of the oral cavity against pathogens (Sumi *et al.,* 2007). Differing from the other alimentary tract-associated glands, the salivary glands are innervated by both sympathetic and parasympathetic nerves, resulting in the constituent secretion of saliva under any physiological condition (Proctor and Carpenter, 2007). Dysfunction of salivary secretion (hyposalivation) causes xerostomia (dry mouth) and sequentially leads to severe dental caries as well as oral mucosal disorders (Featherstone, 2000).

The parotid salivary gland being one of the major salivary glands of domestic animals contributes to substantial amount of saliva secreted into the mouth.

Its function has multifaceted dimension in digestion, as it provide lubrication for eating and supply saliva for pH buffering. The secretion, saliva, contains water, various enzymes, mucopolysaccharides and lubricating glycoproteins. In general, the major salivary glands of the herbivores are better developed than those of the carnivores.

Detail and applied knowledge of anatomy on a regional basis is required to avoid inadvertent nerve damage during surgery. Results of this research can also be used for surgical treatment of salivary fistula by ligation of Stenson's (parotid) duct in buffalo.

In the literature, the structure of parotid salivary gland of postnatal goat (Elewa, 2010), prenatal buffalo (Singh and Singh, 2014) and postnatal sheep (Singh *et al.,* 2015) has been studied at both macroscopic as well as microscopic levels, but the parotid salivary gland of neonatal buffalo have received little attention, especially from the gross morphological and histomorphochemical point of view. The purpose of the present study is to provide more information about the gross anatomical, histological and histochemical features of the parotid salivary gland of buffalo neonates.

MATERIALS AND METHODS

Collection and fixation of samples

The present study was conducted on parotid salivary gland of eighteen buffalo neonates, in different stages of neonatal development and these stages were classified into three groups: Group-1: <1 month; Group-2: between 1-2 months and Group-3: between 2-3 months. Age of neonates was estimated by their dentition. The head of neonates were fixed in 10 per cent neutral buffered formalin (NBF). After complete fixation the dissection was done. The skin over the gland was incised and fascia was transected. The topography of the parotid salivary gland was studied. The gland was carefully excised from the adhering tissue and the length, breadth and weight of gland were measured on two sides (left and right) and then compared. After gross observations, tissue samples were collected from the parotid salivary gland neonates buffalo, and fixed in 10 per cent neutral buffered formalin (NBF) for 48 hours.

Processing and staining

The tissue samples were processed for paraffin sectioning (5-6 µm thickness) and frozen sectioning (10-12 µm thickness) techniques. These sections were stained with Haematoxylin and Eosin for general histomorphology, Masson's trichrome stain for collagen fibres, Gridley's method for reticular fibres, Verhoeff's method for elastic fibres, Holme's method for nervous tissue, Alcian blue stain (at pH 1.0 and 2.5) for acidic mucopolysaccharides, Periodic Acid Schiff's (PAS) method for neutral mucopolysaccharides, Combined PAS-Alcian Blue method for mucosubstances, Colloidal iron method for acidic mucopolysaccharides, Mayer's mucicarmine method for mucin, Best's carmine stain for glycogen, Sudan black 'B' method for lipids and Oil-red-o method for lipids (Luna, 1968). Lipids and phospholipids were demonstrated on fresh cryostat sections.

Micrometry and statistical analysis

The diameter of serous acini, intercalated ducts, striated ducts and large excretory ducts of parotid salivary gland was measured. The data was tabulated and statistically analysed.

RESULTS AND DISCUSSION

Gross morphological observations

The colour of the parotid salivary gland varied from light yellow to light brown in 8-day-old buffaloes. The lobules of the gland were distinctly visible at this stage of neonatal life. In 19-day-old buffaloes, the dorso-anterior part of the gland was loosely attached to the parotid lymph node, while the ventro-anterior part was in close contact with the masseter muscle. The middle part of the gland was penetrated by the maxillary vein from lateral to medial surface. The lateral surface was covered by parotid fascia, developing parotido-auricularis muscle and facial muscles. The medial surface was uneven and related to great cornu of hyoid bone, digastricus, occipito-hyoideus and sterno-mastoideus muscles, external carotid artery, external jugular vein and its tributaries, facial nerve and its branches. The dorsal border was related to the base of the external ear. The cranial border was in contact

with the parotid lymph node above and masseter muscle below. The caudal border was related to the posterior auricular vein. The facial nerve was also very superficial. The left parotid gland of first group, on an average measured 3.25±0.5 cm in length and 2.85±0.2 cm in breadth whereas the right one was 3.30±0.5 cm in length and 2.88±0.2 cm in breadth. The mean weight of left and right parotid glands was 11.75±1.1 gm and 12.90±1.1 gm, respectively.

In 44-day-old buffalo calves, the parotid gland was long, narrow, pinkish brown in colour and triangular in shape with a wide thick dorsal end that reached the region of the temporo-mandibular joint. However, the gland was reported to be rectangular in sheep and goat (Dellmann and Eurell, 1998).

In 74-day-old buffalo calves, the gland was located along the caudal border of the masseter muscle and extended from the zygomatic arch to the ramus of the mandible. The ventral aspect followed the caudal border of the mandible and was deeply related to the mandibular salivary gland. The deep surface was related to the angle of the stylohyoid bone as well as the occipito-hyoideus and digastric muscles (Fig. 1).

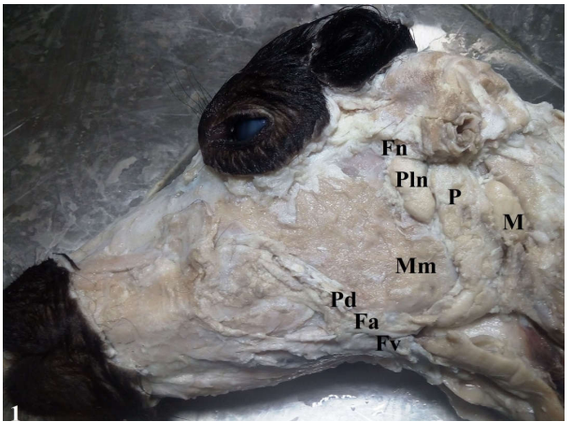

Fig. 1. Photograph of neonatal buffalo head showing distinct lobulations of triangular shaped parotid gland (P). (M-mandibular gland; Fn-facial nerve; Pln-parotid lymph node; Mm-masseter muscle; Pd-parotid duct; Fa- facial artery; Fv- facial vein)

Similar finding was reported in postnatal sheep (Singh *et al.,* 2015). The parotid duct left the gland ventrally with the facial artery as well as facial vein and ascended on the lateral surface of the masseter muscle to open near the posterior upper molar teeth in the oral cavity. The parotid gland of carnivorous mammals including dog and cat is grossly similar to the parotid gland in other mammalian species, but histologically it is seromucous (Dellmann and Eurell, 1998).

The morphometric studies revealed that on an average left parotid gland of this stage buffalo was 5.50±0.8 cm in length, 3.00±0.2 cm in breadth and weighed 19.7±1.5 gm whereas right one was 5.80±0.8 cm in length, 3.10±0.2 cm in breadth and weighed 20.9±1.5 gm. Gradual increase in length, breadth and weight of the gland was due to increased proliferation of ducts, increased lobulation and connective tissue formation during this stage of neonatal buffalo.

There was significant difference in the biometrical parameters of parotid gland between different neonatal age groups at $p \leq 0.05$. The biometrical studies showed that there was no significant difference in the left and right parotid salivary gland within same group at $p \leq 0.05$.

Histomorphological and histochemical observations

In 8-day-old buffaloes, the acinar cells were lined by single layer of epithelium. The epithelial lining cells were pyramidal in shape. The cytoplasm was eosinophilic in nature. The nucleus was spherical and situated towards the basal surface of the cells. The myoepithelial cells appeared as flattened basal cells initially around the developing acinar cells, as reported in sheep parotid gland (Singh *et al.,* 2015). The capsule was well developed around the gland and the lobulation of the gland was completed in 19-day-old buffalo. The typical compound tubuloacinar nature and dense compact lobulation of the gland with branched bush like network formation was attained at this stage and there was an increase in the number of lobules (Fig. 2).

The parotid gland of sheep was consisted of compound tubules being surrounded by collagenous connective tissue capsule (Muthukrishnan, *et al.,* 2013). Purely serous acinar cells were observed in the parenchyma of gland with spherical nuclei located near the centre of the cell. In organ developmental study of salivary glands of miniature pig, the parotid gland is purely serous in nature (Zhou, *et al.,* 2010).

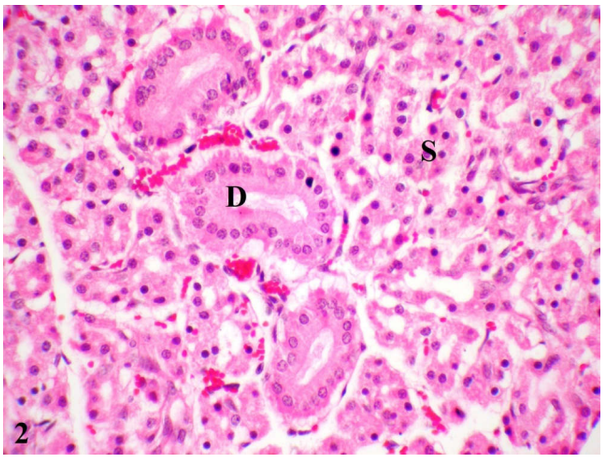

Fig. 2: Photomicrograph of parotid salivary gland of 19-day-old buffalo calf showing predominantly serous acini (S) along with several orders of ducts (D) distributed in the stroma (Haematoxylin and Eosin method × 400).

The parotid gland of European hamster was found to be of the purely serous type, in association with intercalated and striated ducts (Khojasteh and Delashoub, 2012). However, the gland was reported to be of mixed type in young puppies and lambs (Dellmann and Eurell, 1998). Infiltration of lymphocytes was observed in intralobular space. In interlobular space, fine elastic fibres were seen in the wall of blood vessels.

The serous acini lacked sulphomucin content while goblet cells were strongly positive at this stage of neonatal development. Large ducts with goblet cells also showed strong positive reaction to neutral mucopolysaccharides, however, secretory acinar cells were devoid of these mucopolysaccharides (Fig. 3).

Similar type of reaction was observed in parotid gland of sheep (Singh *et al.,* 2015). Goblet cells showed mixed activity for neutral and acidic mucopolysaccharides. Localization of neutral mucopolysaccharides in acinar cells of bovine parotid gland was noticed, whereas these cells lacked acidic mucopolysaccharide content (Lemmon, 2008).

Weak protein activity was observed in this group, however, moderate activity was observed in blood vessels. Secretory cells of the gland lacked glycogen as confirmed by Best carmine method.

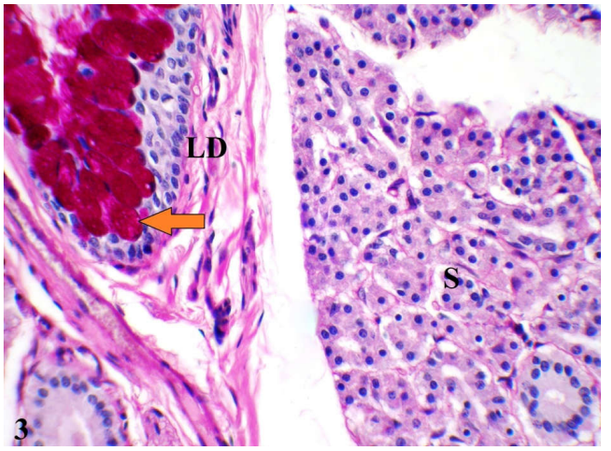

Fig. 3: Photomicrograph of parotid salivary gland of 19-day-old buffalo showing serous cells (S) devoid of neutral mucopolysaccharides, however, goblet cells (arrow) in the large duct (LD) strongly positive (Periodic Acid Schiff's method × 400)

Fine Sudanophilic lipid droplets were also observed in the interlobular connective tissue ((Fig. 4), as reported in sheep parotid gland (Muthukrishnan, *et al.,* 2013).

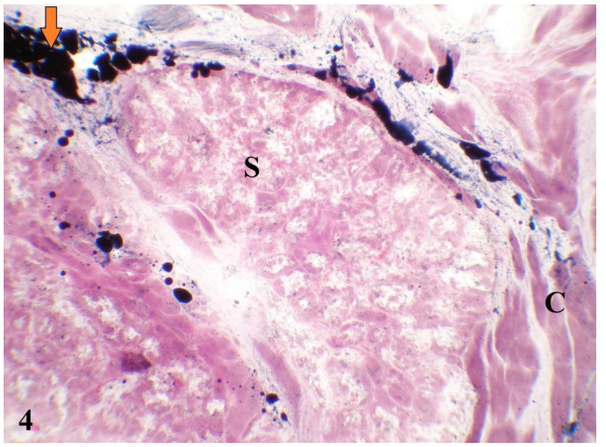

Fig. 4: Photomicrograph of 19-day-old buffalo parotid gland showing presence of fine lipid droplets (arrow) in the interlobular connective tissue (S-serous acini; C-capsule) (Sudan Black B method × 100)

The lipid droplets increased and were comparatively coarse in duct epithelium. Some adipose connective tissue was seen in glandular stroma. Moderate amount of phospholipids were observed in the cell membrane

of secretory cells and ducts. These phospholipids constituted the main component in plasma membrane of all the cells and thereby play an important role in formation of cell membrane (Kishore *et al.,* 1998). In this group, the mean diameter of serous acini, intercalated duct, striated duct and large excretory duct were 1.49+0.1 µm, 1.18+0.1 µm, 2.21+0.1 µm and 4.95+0.1 µm, respectively. With the advancement of age, the diameter of the acini increased and amount of connective tissue decreased.

In 44-day-old buffaloes, the parotid gland was surrounded by a thick connective tissue capsule made of dense collagen fibres along with few elastic and reticular fibres. Similar finding was reported in goat parotid gland (Muthukrishnan, *et al.,* 2014). The connective tissue traversed the gland to form septae and separated the glandular parenchyma into lobes and lobules. This finding was in total agreement with that reported in goat (Muthukrishnan*, et al.,* 2014).

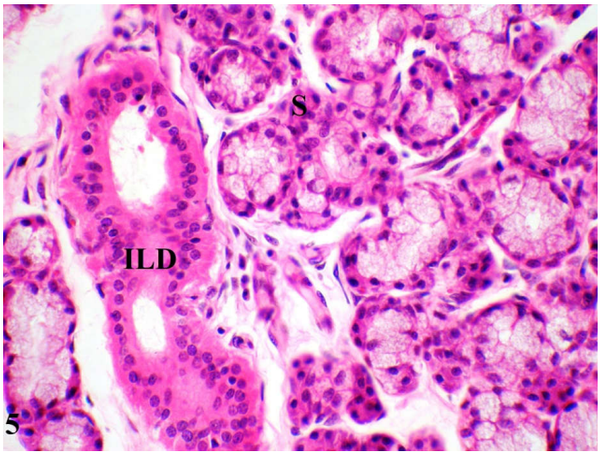

Fig. 5: Photomicrograph of parotid salivary gland of 44-day-old buffalo showing parenchyma comprised of purely serous cells (S) along with intralobular duct (ILD) distributed in the stroma (Haematoxylin and Eosin method × 400).

The radiating septae that separated the lobes and lobules of the parenchyma were noticed in the parotid gland of sheep and it was surrounded by collagenous connective tissue capsule (Vignoli and Nogueira, 2007). The parenchyma of the parotid gland comprised of purely serous acini along with several orders of ducts distributed in the stroma (Fig. 5). In Zebus (*Bos indicus*), the parotid salivary gland was entirely serous in older animals, but mucous end pieces were reported in younger animals (Lemmon, 2008). Each serous acinus comprised of approximately four to six pyramidal cells and enclosed a distinct lumen. The pyramidal cells of serous acini were acidophilic with basal spherical nuclei (Fig. 5). Distinct elastic fibres were also observed in the septa as well as in the blood vessels of the stroma (Fig. 6).

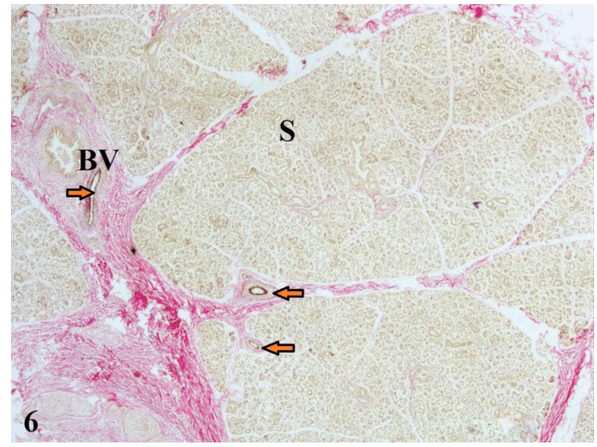

Fig. 6: Photomicrograph of 44-day-old buffalo parotid gland showing presence of distinct elastic fibres (arrows) in the septa as well as in the blood vessels (BV) of stroma (S-serous acini) (Verhoeff's method × 40).

Large plexus of ganglion cells and blood vessels were also noticed in the capsule from which nerve fibrils traversed through the septa and ramified along the basement membrane of the acini and ducts.

The lobules became larger and showed a marked increase in the number of acini and a reduction in intralobular connective tissue in 74-day-old buffaloes. These results corroborated well with the findings in sheep in which 86 per cent of parenchyma consisted of acinar secretory cells than other ducts and cellular elements (Singh *et al.,* 2015). Increase in the acinar cells completely filled the parenchyma. The serous acini were surrounded by myoepithelial cells, connective tissue stroma and ducts of various orders. The same type of arrangement was noticed in the parotid gland of dog (Dellmann and Eurell, 1998), goat (Muthukrishnan*, et al.,* 2014), sheep (Elewa *et al.,* 2010). The myoepithelial cells were scattered around the serous acini as well as the intercalated and

striated duct of the parotid gland. These were dark basophilic in nature. The myoepithelial cells lining the duct epithelium appeared spindle shaped with few cytoplasmic processes. The acini were surrounded by stellate shaped myoepithelial cells, connective tissue and ducts of various orders in goat (Muthukrishnan, *et al.,* 2014). Lipofuscin pigments were observed in the stroma of parotid gland at this stage of neonatal development.

The duct system of the parotid gland was comprised of intercalated duct, striated duct, interlobular duct and large excretory duct. The ducts of various orders predominated the secretory parenchyma at this stage. The serous acini first opened into small intercalated ducts, lined by cuboidal epithelium as reported in parotid gland of sheep (Singh *et al.,* 2015). The intercalated ducts, with defined morphology, were short with little cytoplasm delimiting a very small lumen. The intercalated duct opened into large striated ducts within the lobules. In contrary to the above finding, the intercalated duct in domestic animals was lined by simple columnar epithelium (Dellmann and Eurell, 1998).

The striated ducts, with morphology close to that of the adult animal, were seen long, with a wide lumen, and consisted of prismatic cells already exhibiting the characteristic longitudinal striations in the basal third and central spherical nuclei. The striated ducts were lined by simple columnar epithelium. The cytoplasm of the cells lining the striated ducts was eosinophilic, while the nuclei were basophilic and darkly stained. The striated duct extended to the periphery of the lobule to open into interlobular ducts (Fig. 5). In buffalo calves, the striated ducts occurred in groups and lacked distinct striations (Lemmon, 2008). Several interlobular ducts opened into large excretory duct where the epithelium changed from pseudostratified columnar to stratified squamous epithelium. Presence of myoepithelial cells surrounding the intercalated duct was considered as a distinguishing feature to identify these ducts in goat parotid gland (Elewa *et al.,* 2010).

The larger ducts situated in the stromal tissue within the lobule and in between the lobes and were lined by pseudostratified columnar epithelium and showed basal cells and also few goblet cells in between the columnar cells. With the advancement of age, the striated and excretory ducts seemed to have increased in size. The differentiation of the secretory elements of parotid gland of sheep occurred in later neonatal age and continued postnatally (Vignoli and Nogueira, 2007).

The serous cells and the stroma of gland showed negative reaction for acidic mucopolysaccharides. The acinar cells also lacked neutral mucopolysaccharide content however; goblet cells in the large duct were intense PAS positive which revealed the presence of large amount of neutral mucopolysaccharides during this stage. Combined PAS-AB method showed strong mixed reaction for acidic and neutral mucopolysaccharides in goblet cells, while moderate alcianophilic reaction was observed in connective tissue (Fig. 7). However, a few mucous secreting cells with intense positive reactions for both PAS and AB stains were noticed in the distal portions of the interlobular ducts in the parotid gland of sheep (Singh *et al.,* 2015). Strong activity of sulphomucins was observed in large ducts.

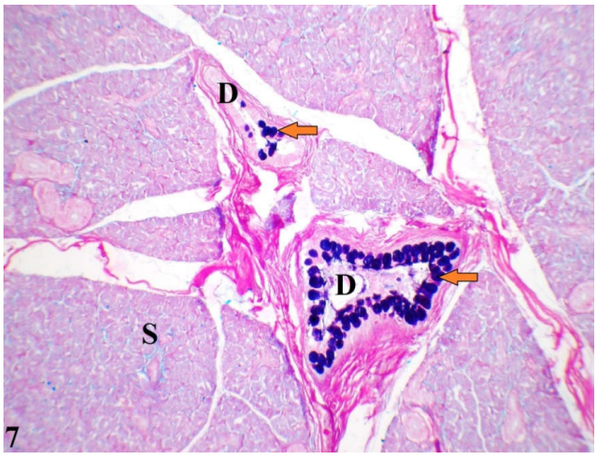

Fig. 7: Photomicrograph of parotid salivary gland of 74-day-old buffalo showing mixed reaction in goblet cells (arrows) of large ducts (D), serous cells (S) devoid of reaction (Combined Periodic Acid Schiff's–Alcian Blue method × 100).

Large ducts showed strongly positive reaction for mucinous substances. Colloidal iron method showed negative reaction for acidic mucopolysaccharides in serous acinar cells and ducts, however moderate reaction was found in connective tissue (Fig. 8).

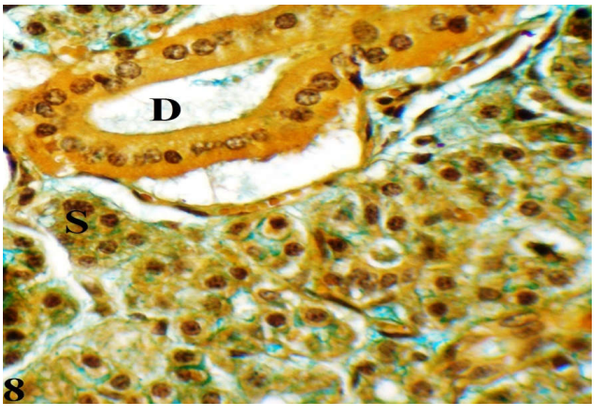

Fig. 8: Photomicrograph of 74-day-old buffalo parotid gland showing serous cells (S) and ducts (D) devoid of acidic mucopolysaccharides, moderate reaction in connective tissue (Colloidal Iron method × 400).

Fat globules were noticed in the epithelium of ducts by Oil-red-O method, however, secretory acinar cells showed weak reaction (Fig. 9).

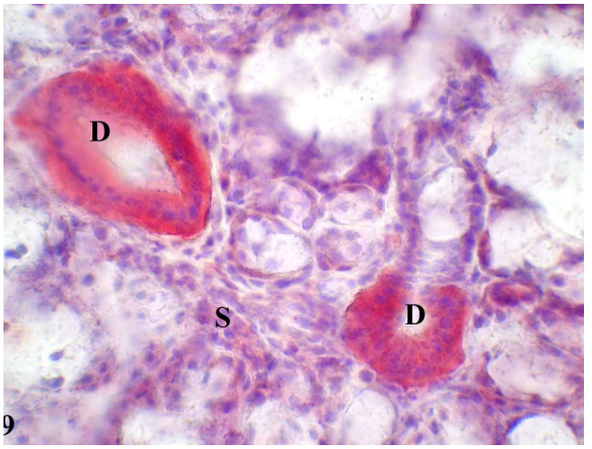

Fig. 9: Photomicrograph of parotid salivary gland of 74-day-old buffalo showing presence of fat globules in the epithelium of ducts (D), and weak reaction in secretory cells (S) (Oil-red-O method × 200).

The mean diameter of serous acini, intercalated duct, striated duct and large excretory duct, at this stage of neonatal life was 1.70+0.1 µm, 1.37+0.1 µm, 3.71+0.1 µm and 6.92+1.2 µm, respectively. There was significant difference in the micrometrical parameters of parotid gland between different groups at $p < 0.05$.

CONCLUSION

It may be concluded that there was a significant difference in the biometrical parameters of parotid gland between different neonatal age groups at $p \leq 0.05$ and $p \leq 0.01$ level, however there was no significant difference in the left and right parotid salivary gland within same group at $p \leq 0.05$ and $p \leq 0.01$ level. Gradual increase in length, breadth and weight of the gland was due to increased proliferation of ducts, increased lobulation and connective tissue formation during development of neonatal buffalo. The typical compound tubuloacinar nature and dense compact lobulation of the gland with branched bush like network formation was attained at early neonatal stage. The parenchyma was comprised of purely serous acini along with several orders of ducts distributed in the stroma. The duct system was comprised of intercalated duct, striated duct, interlobular duct and large excretory duct. The myoepithelial cells appeared as flattened basal cells initially around the developing acinar cells. The serous acinar cells of parotid gland were devoid of acidic as well as neutral mucopolysaccharides in neonatal age groups. Some adipose connective tissue was seen in glandular stroma. There was significant difference in the micrometrical parameters of parotid gland between different groups at $p \leq 0.05$ and $p \leq 0.01$ level.

ACKNOWLEDGEMENTS

We are thankful to Guru Angad Dev Veterinary and Animal Sciences University (GADVASU), Ludhiana for providing all type of facilities to carry out the study. The funding was provided by Department of Science and Technology (DST), New Delhi, Government of India for research under INSPIRE program (DST-INSPIRE Fellowship, IF 120277).

REFERENCES

Amano, O. 2011. *The salivary gland: Anatomy for surgeons and researchers*. *Jpn. J. Oral Maxillofac. Surg.*, **57**: 384-393.

Dellmann, H.D. and Eurell, J.A. 1998. *Digestive System. In: Text book of Veterinary Histology*. 5th Ed., William and Wilkins, London, pp. 174-176.

Elewa, Y.H., Bareedy, M.H., Abudatta, A.A, Ichii, O., Otsuka, S., Kanazawa, T., Lee, S., Hashimoto, Y. and Kon, Y. 2010.

Structural characteristics of goat (*Capra hircus*) parotid salivary glands. *J. Vet. Res.,* **58**: 121-135.

Featherstone, J.D. 2000. The science and practice of caries prevention. *J. Amer. Dent. Assoc.,* **131**: 887–899.

Khojasteh, S.M.B. and Delashoub, M. 2012. Microscopic anatomy of the parotid and submandibular salivary glands in European hamster (*Cricetus cricetus L.). Int. Res. J. Appl. Basic Sci.*, **3**: 1544-1548.

Kishore, P.V.S., Sundararao, K.V. and Gopinath, S. 1998. Histological and histochemical studies on the parotid salivary gland of goat (*Capra hircus*). *Ind. J. Vet. Anat.*, **10**: 88-89.

Lemmon, M.A. 2008. Membrane recognition by phospholipid-binding domains. *Nat. Rev. Mol. Cell Biol.,* **9**: 99-111.

Luna, L.G. 1968. *Manual of histologic staining methods of the armed forces institute of pathology.* 3rd Ed., McGraw Hill Book Co., New York.

Muthukrishnan, S., Basha, S.H, Ramesh, G., Ushakumary, Kumaravel, A. and Rajathi, S. 2014. Histogenesis of parotid salivary gland in sheep (*Ovis aries*). *Ind. Vet. J.,* **91**: 40-42.

Muthukrishnan, S., Basha, S.H., Ramesh, G., Ushakumary, Rajathi, S. and Kumaravel, A. 2013. Histomorphology of parotid salivary gland in sheep (*Ovis aries*). *Ind. J. Vet. Anat.,* **25**: 92-93.

Proctor, G.B. and Carpenter, G.H. 2007. Regulation of salivary gland function by autonomic nerves. *Auton. Neurosci*., **133**: 3-18.

Singh, A.D. and Singh, O. 2014. Histoenzymic studies on parotid salivary gland of buffalo during prenatal development. *Ind. J. Vet. Anat.,* **26**: 110-112.

Singh, A.D., Jain, R.K. and Kumar, P. 2012. Histomorphological and histochemical studies on the dorsal buccal gland of sheep (*Ovis aries*). *Ind. J. Vet. Anat.,* **24**: 26-28.

Singh, A.D., Sasan, J.S., John, M.A. and Choudhury, A.R. 2015. Gross and microscopic characterization of the parotid salivary gland of sheep. *Ind. Vet. J.* **92**: 61-63.

Sumi, M., Yamada, T., Takagi, Y. and Nakamura, T. 2007. MR Imagine of labial glands. *Amer. J. Neuroradiolog*., **28**: 1552-1556.

Vignoli, V.V. and Nogueira, J.C. 2007. Histology and mucosubstance histochemistry of the parotid gland in suckling, prepuberal and puberal zebus (*Bos indicus*). *Anat. Histolog. Embryolog.,* **10**: 147-158.

Zhou, J., Wang, H., Yang, G., Wang, X., Sun, Y., Song, T., Zhang, C. and Wang, S. 2010. Histological and ultrastructural characterization of developing miniature pig salivary glands. *Anat. Rec.,* **293**: 1227-1239.